A New Coronagraph for NAOS–CONICA — the Apodising Phase Plate

Matthew Kenworthy[1]
Sascha Quanz[2]
Michael Meyer[2]
Markus Kasper[3]
Julien Girard[3]
Rainer Lenzen[4]
Johanan Codona[5]
Philip Hinz[5]

[1] Leiden Observatory, the Netherlands
[2] ETH Zurich, Switzerland
[3] ESO
[4] Max-Planck-Institut für Astronomie, Heidelberg, Germany
[5] University of Arizona, USA

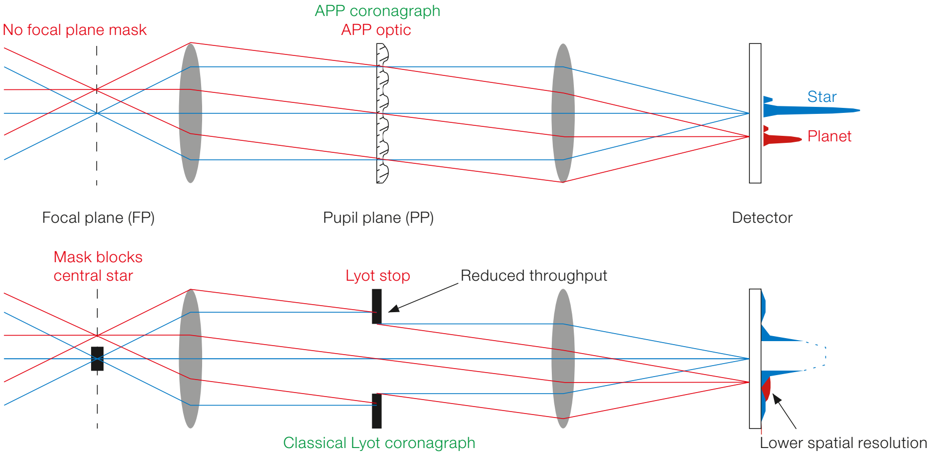

Figure 1. A comparison of the principles used in the Apodising Phase Plate coronagraph and in a classical Lyot coronagraph.

In April 2010, a new coronagraphic optical element, called an Apodising Phase Plate (APP), was installed in NAOS–CONICA (NACO). The APP coronagraph is optimised for use at 4.05 μm with both narrow- and broadband filters. Unlike other types of coronagraph, it requires no alignment overhead and can be used immediately after switching from direct imaging for observing targets of interest where high contrast is required.

The Apodising Phase Plate (APP) is optimised for observations using the newly introduced IB4.05 filter in NACO (Rousset et al., 2003; Lenzen et al., 2003) and we have also demonstrated its performance at broader bandpasses around 4 μm with the *L′* filter (Kenworthy et al., 2010). In this article, we describe the principle of the optical element, how it can be used for NACO observations and explain its strengths and weaknesses.

The goal of a coronagraph is to minimise the diffracted light from one astronomical source whilst letting through as much of the light as possible from a nearby, usually much fainter, source. The original Lyot coronagraph uses two optical elements within an astronomical camera to suppress light from the on-axis source. The image of the central star and a nearby planet, for example, is formed in a focal plane (FP), where a mask blocks light from the star out to a given radius (see Figure 1). The planet is ideally displaced off to one side of the star, and the light from the planet is not blocked by this mask. Reimaging optics form a pupil plane (PP) image (often coincident with the camera's filter wheel) and a Lyot stop then blocks light from the outer edge of the re-imaged telescope pupil, before going on to form the final image using another optical element at the science detector. Kasper et al. (2009) described pupil-stabilised Lyot coronagraphy at 4 μm with NACO for exoplanet detection. The classical Lyot design is sensitive to the telescope's alignment of the star on the focal plane mask and there is a strong trade-off between angular resolution and achievable suppression: if the planet is too close to the star, the planet's light can also be blocked by the focal plane mask. Other coronagraphic designs, such as the four quadrant phase mask and phase-induced amplitude apodisation, significantly improve on the Lyot design, but still suffer from the tight tip-tilt alignment tolerances in the focal plane (for a review comparing many types of coronagraph, see Guyon et al., 2006).

How the APP works

The Apodising Phase Plate consists of just one optical element, rather than two, in the pupil plane of the telescope. It is a development of phase apodisation coronagraphy, originally developed by Johanan Codona at the University of Arizona (Codona & Angel, 2004; Codona, 2006) and initially tested at the 6.5-metre MMTO (Kenworthy et al., 2007). Here, we use light diffracted from the Airy core of the central star to cancel out the coherent light in the outer diffraction rings. Small sinusoidal ripples of phase added to the incoming wavefront act like a simple diffraction grating, creating a pair of "speckles" that can be adjusted to cancel out diffraction on one side of the star, but reinforcing it on the opposite side. Mathematically adding many of these virtual gratings together forms the resultant APP pattern, seen in Figure 2. Its effect on the Very Large Telescope (VLT) point spread function (PSF) is seen in the commissioning data in Figure 3. The APP optical element itself is shown in Figure 4 prior to installation.

It is important to note that every imaged object in the field of view — including any faint companions and extended structure — all have this new, modified APP PSF. Since energy from the Airy core is used in suppressing diffraction, there is an effective loss of transmission of the faint companion. We have designed the plate to use 40 % of the Airy core flux to provide diffraction suppression, but this loss of planet flux is more than compensated by the much larger reduction of diffracted light from the central star. The measured throughput for the APP is 0.60 with an error of 0.02, consistent with the design specifications.

Since there is no focal plane mask that the target star has to be aligned behind, the greatest benefit for a NACO user is that there is no alignment overhead for the APP coronagraph. The target star can be beam-switched anywhere on the imaging array with no impact whatsoever on the

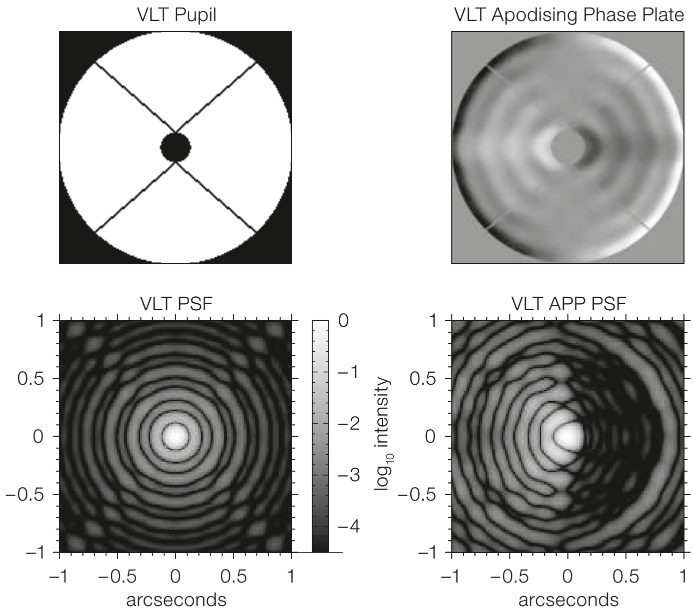

Figure 2. (Left) The APP phase plate pattern and its effect on the VLT point spread function.

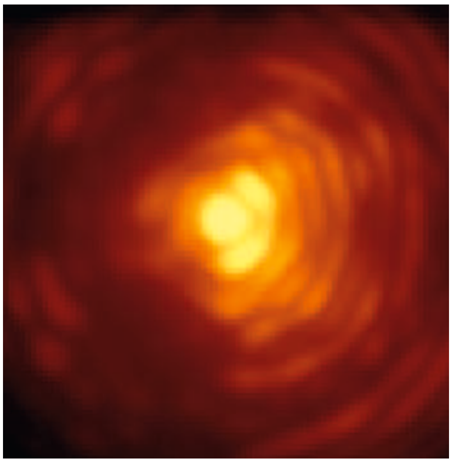

Figure 3. (Right) An image of the VLT PSF taken with the APP on NACO. The image has been logarithmically scaled for clarity.

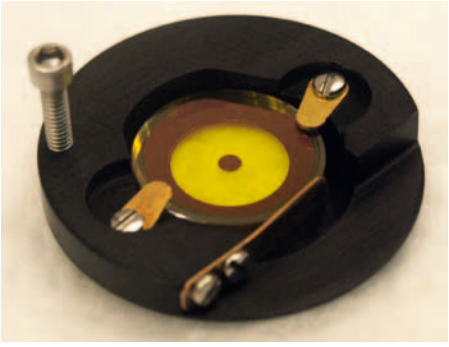

Figure 4. The APP optical element prior to installation in CONICA. The light yellow area is the transmissive ZnSe and the brown area is a gold coating that aids alignment in the pupil mask wheel.

coronagraph's performance. All coronagraphs represent a trade-off between inner working angle, planet flux throughput, and spatial resolution. In the case of the APP, it is designed to provide diffraction suppression from 0.180 arcseconds out to 0.750 arcseconds, moving the sky background limit up to three times closer to the central star than direct imaging observations. Beyond a radius of 0.750 arcseconds (the actual value varies with target star magnitude and adaptive optics [AO] correction) it is preferable to use direct imaging and related subtraction techniques.

Using the APP with NACO

The APP is used with the CONICA L27 camera nominally providing a field of view of 28 by 28 arcseconds. However, to prevent ghost reflections from the optics interfering with the coronagraphic mode, the APP has an optical wedge introduced into it. The practical result is that the APP can be used over the upper third of the detector area (i.e. no restrictions along the *x*-axis of the detector). There is no impact on the PSF quality and one can beam-switch along this part of the detector in a manner identical to direct imaging observational techniques. Observing with the APP does not increase the overhead of observations apart from that due to the reduced coronagraphic throughput of 60 %. If full field coverage around a target of interest is required, a second dataset with the field of view rotated by 180 degrees is required to cover both hemispheres around a target.

The APP can be used in pupil-tracking mode so that the fixed-pattern speckles of the telescope and instrument remain fixed with respect to the orientation of the APP PSF. A combination of angular differential imaging and/or PSF subtraction with a nearby reference star with similar colour and magnitude is required to minimise contributions from the uncorrected seeing halo produced by the adaptive optics system and to minimise any residual quasi-static speckles. The APP optical element is chromatic and is designed for a central wavelength of 4.05 μm, but the coronagraphic suppression only degrades slowly with increasing bandwidth, which was seen in the *L′* contrast curve determined during engineering time in April 2010.

In Figure 5, we show the contrast achieved in a 30-minute integration on HIP 61460 (an F2 V star with $L' = 6.2$ mag) using the *L′* filter (central wavelength 3.8 μm) with the observations made in pupil-tracking mode with detector integrations of DIT = 0.175 s, NDIT = 30 and NINT = 5, yielding five images at different dither positions. All images were in the linear detector regime (approximately one-third full well), the DIMM seeing varied between 0.7 and 0.8 arcseconds, and the airmass was less than 1.1. The contrast curve was calculated by stacking the images together and computing the root mean square (rms) per pixel in the stack. Using an aperture with a radius of 5 pixels, the mean flux per pixel in the core of the PSF was computed and then divided by the mean flux per pixel for a planet with a signal-to-noise ratio of 5 (estimated from the rms in a similar aperture at a given radial separation). The resultant *L′* contrast curve shows that the APP is working as expected and approximately as predicted from the simulations, and the contrasts are comparable to those from other coronagraphs. The steep drop of the contrast curve shows the specific strength of the APP, as we reach a 5σ point source detection limit of 10 magnitudes at 0.4 arcseconds offset.

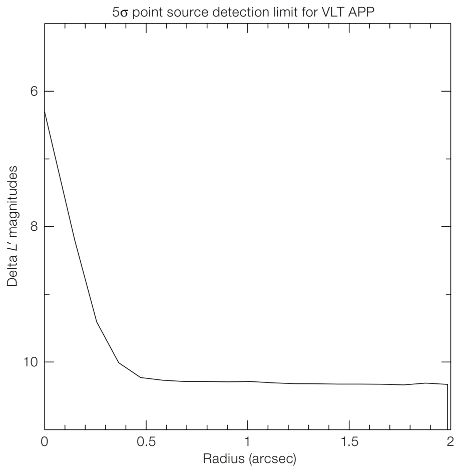

Figure 5. An *L′* contrast curve taken with the APP coronagraph. The curve shows the 5σ detection limit of a point source in *L′*-band as a function of angular separation from a star. The curve is calculated over a 150-degree wedge centred in the high contrast side of the APP PSF.

Further data on a brighter star will be taken to explore the contrast limit at larger radii, as in this dataset we are sky background limited at 0.5 arcseconds offset.

Thermal wavelengths are a natural regime for exoplanet searches, as the planet-to-star flux ratio falls more slowly with effective temperature than at shorter wavelengths (Hinz et al., 2006; Kasper et al., 2007). As telescope apertures increase, the red colours of exoplanets (see Heinze et al., 2010 for a fuller discussion) mean that the *L′*- and *M*-bands become more favourable for direct imaging contrast-limited searches around nearby stars.

The APP is available for general use with NACO, and some of the first results using the APP to obtain NB4.05 photometry of the planet beta Pictoris b (Lagrange et al., 2010) have been submitted (Quanz et al., 2010). Further developments include an achromatised design suitable for working over broader wavelength ranges, and the potential for inclusion on the European Extremely Large Telescope (E-ELT) for thermal imaging of exoplanets with instruments such as METIS (see Brandl et al., 2010).

References

Brandl, B. et al. 2010, The Messenger, 140, 30
Codona, J. & Angel, J. R. P. 2004, ApJL, 604, 117
Codona, J. et al. 2006, SPIE, 6269, 55
Guyon, O. et al. 2006, ApJS, 167, 81
Heinze, A. et al. 2010, ApJ, 714, 1570
Hinz, P. et al. 2006, ApJ, 653, 1486
Kasper, M. et al. 2007, A&A, 472, 32
Kasper, M. et al. 2009, The Messenger, 137, 8
Kenworthy, M. et al. 2007, ApJ, 660, 762
Kenworthy, M. et al. 2010, SPIE, 7735, arXiv:1007.3448
Lagrange, A.-M. et al. 2010, Science, 329, 57
Lenzen, R. et al. 2003, SPIE, 4841, 944
Quanz, S. et al. 2010, ApJL, submitted
Rousset, G. et al. 2003, SPIE, 4839, 140

Credit: ALMA (ESO/NAOJ/NRAO)

Testing of the first two fully assembled European ALMA antennas, manufactured by the AEM consortium, has recently begun at the ALMA Operations Support Facility (OSF). The image shows a European antenna being moved by one of the ALMA transporters, Lore, at the OSF.